

Supplement of

Large seasonal and interannual variations of biogenic sulfur compounds in the Arctic atmosphere (Svalbard; 78.9° N, 11.9° E)

Sehyun Jang et al.

Correspondence to: Kitack Lee (ktl@postech.ac.kr) and Young Jun Yoon (yjyoon@kopri.re.kr)

Text.S1. Independent validation of isotope analysis using black

To investigate the reliability of isotope measurement, we compared black carbon (BC) data with sulfate concentrations during the campaign periods. Arctic Haze, which originates from mostly northern Europe, consists of sulfate and other inorganic compounds, also contains black carbon resulting from incomplete combustion of fossil fuel and burning of forests (Li and Barrie, 1993; Udisti, 2016) and is one of the major sources of aerosols in the Arctic during late winter to early spring (Shaw, 1995; Quinn et al., 2007). It was reported that there are similar seasonal variations and significant correlations between BC and NSS-SO_4^{2-} in the Arctic atmosphere indicating that they have common sources and aging processes of aerosols during meridional transport (Gong et al., 2010; Massling et al., 2015). To estimate the amount of Anth-SO_4^{2-} based on BC data, we first compared NSS-SO_4^{2-} and BC measured in March to April when the effect of Arctic Haze is most intense. Here, we assumed that all of NSS-SO_4^{2-} collected in that period would have Anth-SO_4^{2-} as the dominant contributor. Furthermore, we filtered a few data points (where $\text{Bio-SO}_4^{2-}/\text{total SO}_4^{2-} > 0.2$) to avoid systematic bias in the calculation of the ratio between NSS-SO_4^{2-} and BC. As a result, the value of 17.3 was chosen to represent the correlation of Anth-SO_4^{2-} and BC in the Arctic Ocean and the results are shown in Fig. S1. In spite of the different location of the sampling site (BC measured in Zeppelin observatory; 78.5° N, 11.8° E, 474 m above sea level), the sulfate and BC profiles matched quite well in the spring (March to May). Most of the spring time, we confirmed that those Anth-SO_4^{2-} calculated based on BC concentration and isotope analysis are similar, which indicates the reliability of isotope measurement. When we compare the concentration of Anth-SO_4^{2-} in summer, the difference (or relative amount of Anth-SO_4^{2-}) is getting bigger, which is induced by the different air mass circulation in spring and summer and also the diminishing effect of Arctic Haze in the summer, that is, lower concentrations of Anth-SO_4^{2-} and BC, and also different origins of air masses reflecting different ratios in Anth-SO_4^{2-} and BC. Samples with higher black carbon concentration could be originated from distant regions (i.e. not locally produced, mostly from low-latitude regions) resulting from different environmental conditions, showing different ratios.

Table. S1. Data points excluded for calculation of MSA to Bio-aerosol ratios

Year	Day of year	Bio-SO ₄ ²⁻ (ng m ⁻³)	MSA (ng m ⁻³)	R _{Bio}
2018	80.5	0	5.55	1
	86.5	10.45	4.39	0.30
	92.5	0	12.14	1
	95.5	0	24.60	1
	98.5	14.39	8.78	0.38
	164.5	20.53	28.53	0.58
	179.5	3.13	35.91	0.92
	206.5	5.26	35.91	0.87
2019	102.1	0	23.33	1
	105.0	0	28.11	1
	108.1	0	42.28	1
	111.0	0	28.64	1
	114.0	0	43.05	1
	117.1	13.96	62.69	0.82
	120.0	23.60	48.31	0.67
	219.1	0	33.63	1
	222.1	0	32.44	1
	226.0	0	22.68	1
	228.9	4.66	17.22	0.79
	232.0	17.10	41.52	0.71
	235.0	12.86	33.52	0.72
	238.0	12.61	29.22	0.70
241.0	0	22.06	1	

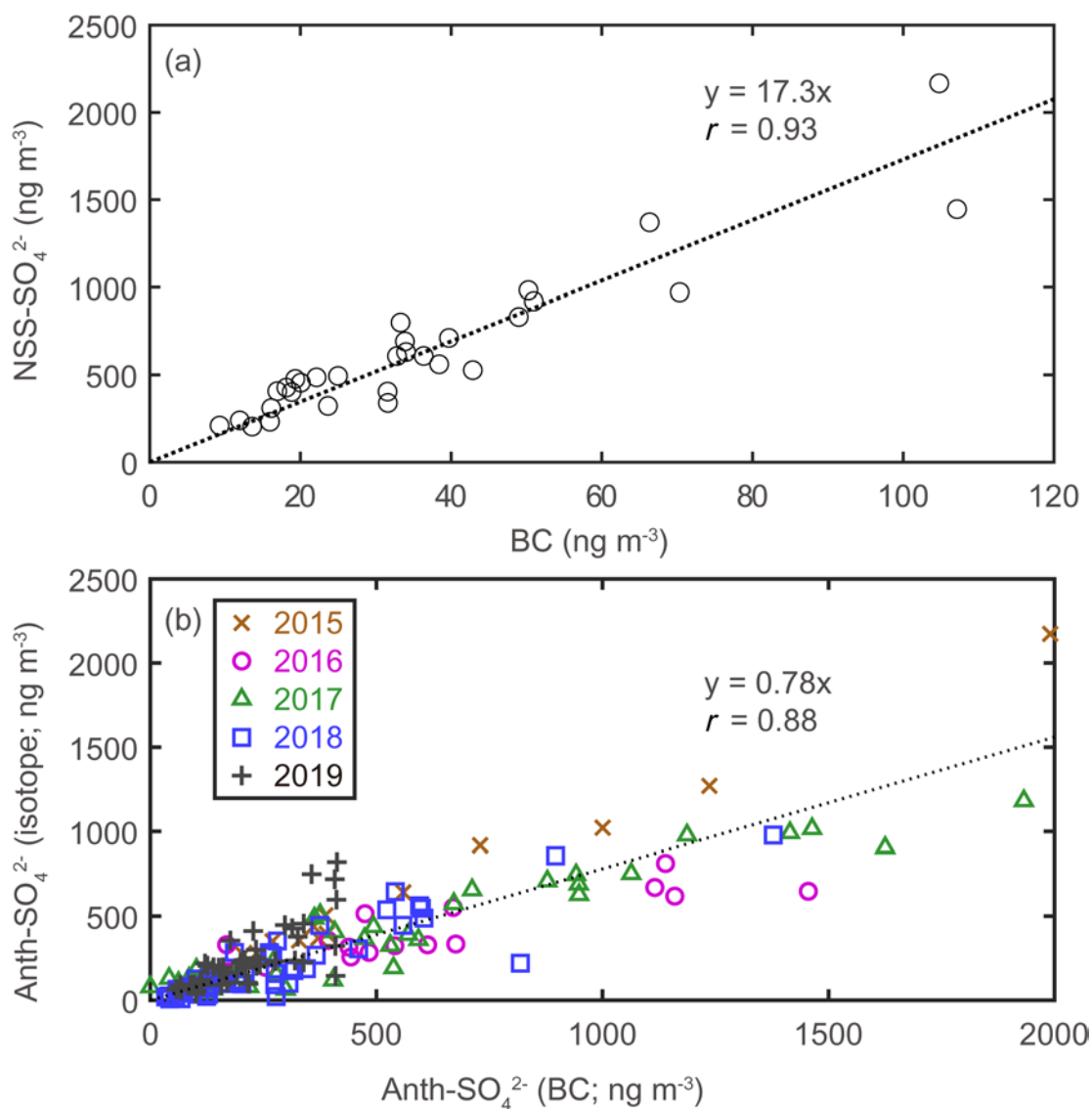


Figure S1: (a) Scatter plot of black carbon (BC) versus NSS-SO₄²⁻ samples collected in March to April (Bio-SO₄²⁻ < 20% of Total SO₄²⁻; n = 23), (b) Scatter plot of Anth-SO₄²⁻ (calculated based on BC concentration) and Anth-SO₄²⁻ (stable isotope measurement results)

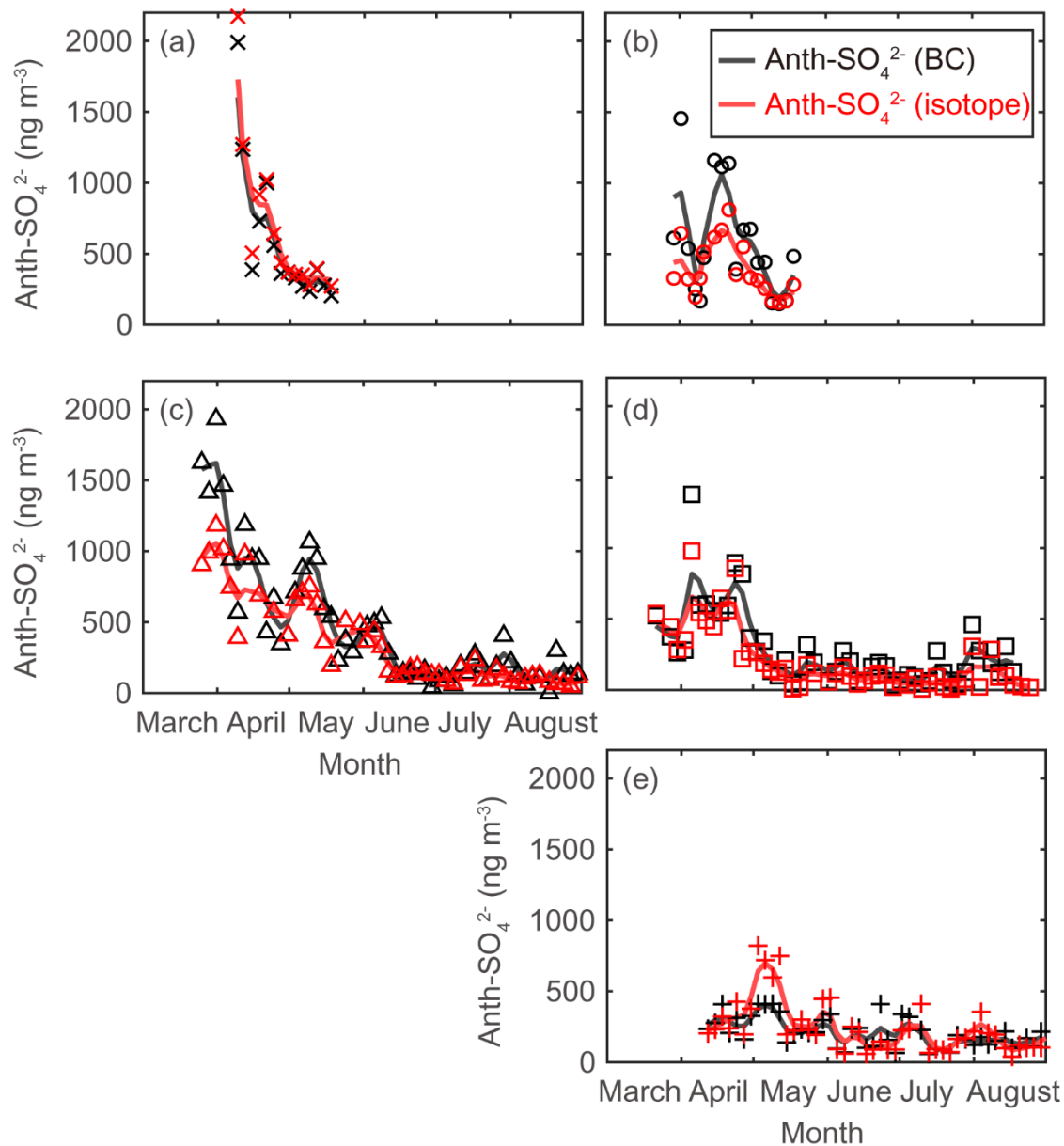


Figure S2: Anthropogenic sulfate concentration estimated by BC concentration (black) stable isotope analysis (red) for (a) 2015, (b) 2016, (c) 2017, (d) 2018, and (e) 2019.

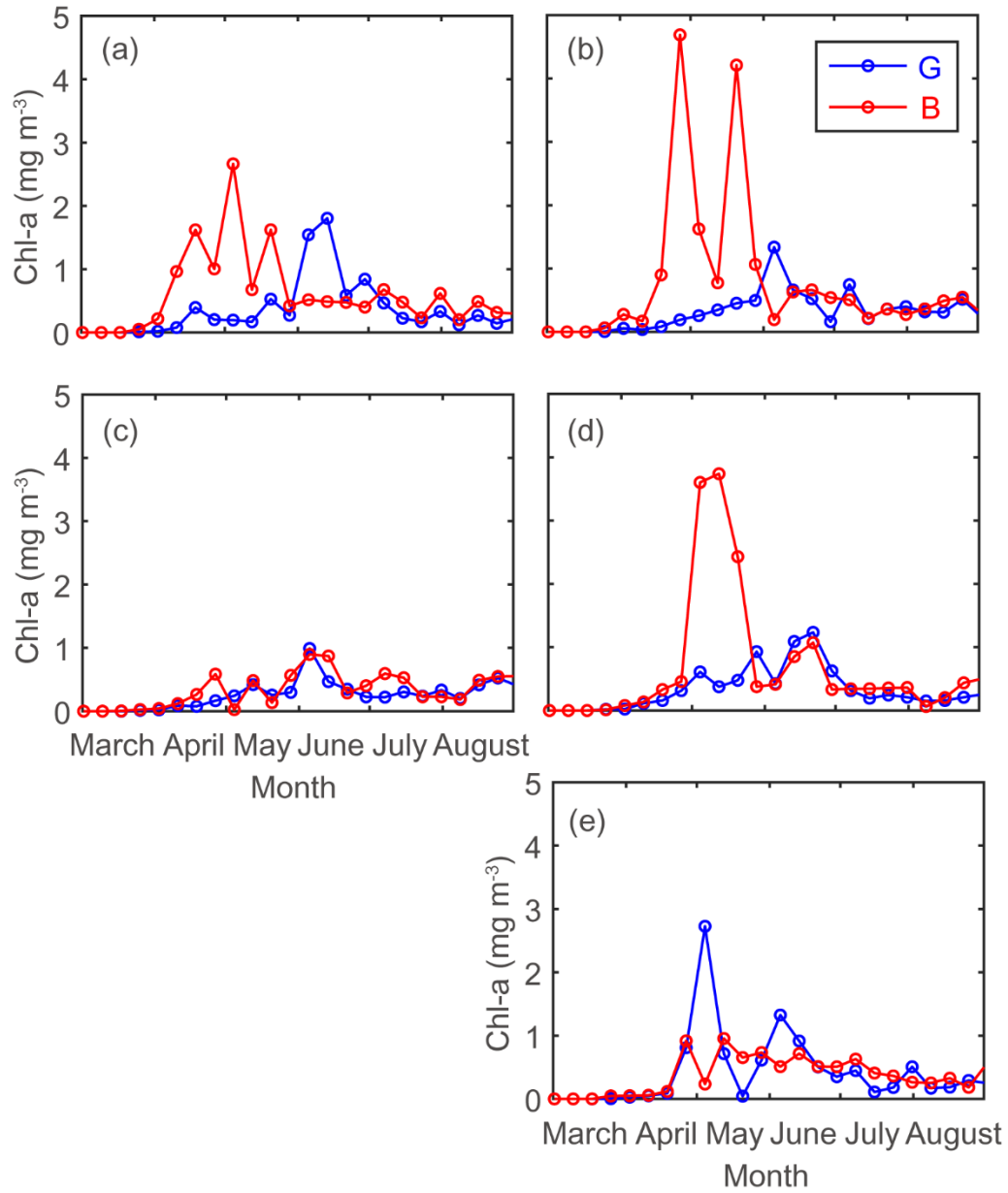


Figure S3: 8-day composite mean concentration of Chl-*a* in Greenland Sea (G; 70° N–80° N, 25° W–16° E; Blue) and Barents Sea (B; 70° N–80° N, 16° E–50° E; Red)

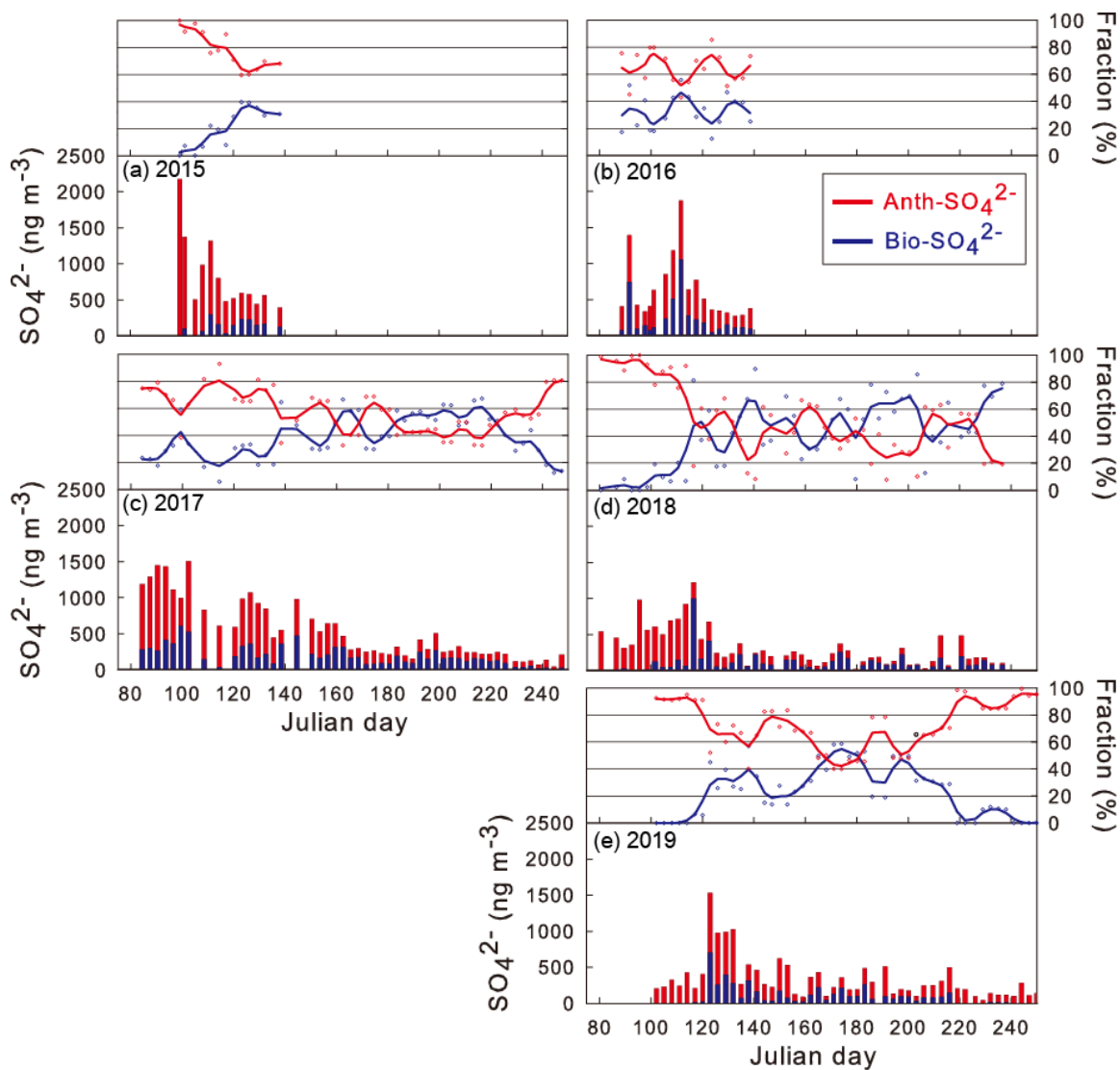


Figure S4: Bar plots showing the concentration of NSS-SO₄²⁻ aerosols (red: Anth-SO₄²⁻; blue; Bio-SO₄²⁻; ss-SO₄²⁻ not shown) for (a) 2015, (b) 2016, (c) 2017, (d) 2018, and (e) 2019.

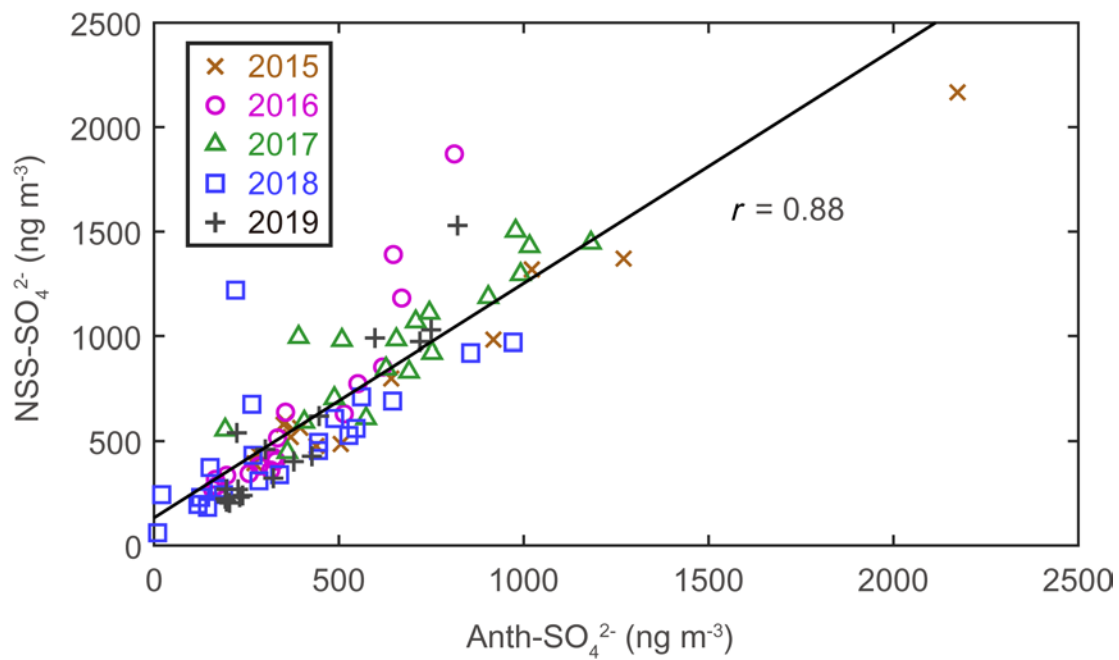


Figure S5: Scatter plot of NSS-SO₄²⁻ versus Anth-SO₄²⁻ from March to May for 2015, 2016, 2017, 2018, and 2019.

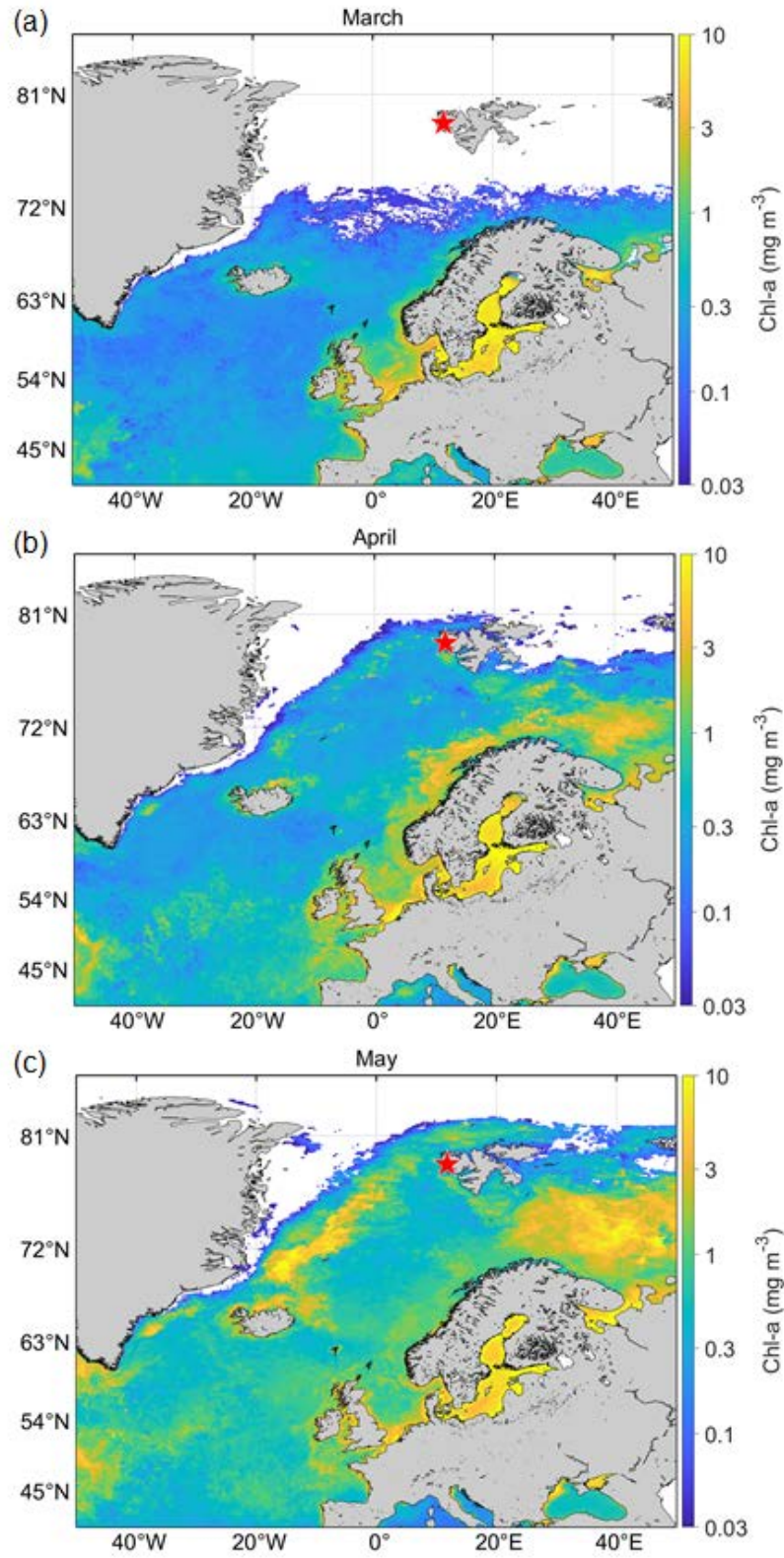


Figure S6: Monthly mean Chl-a concentration in the Arctic Ocean for 2015, 2016, 2017, 2018 and 2019. Red pentagram indicates the location of the sampling site.

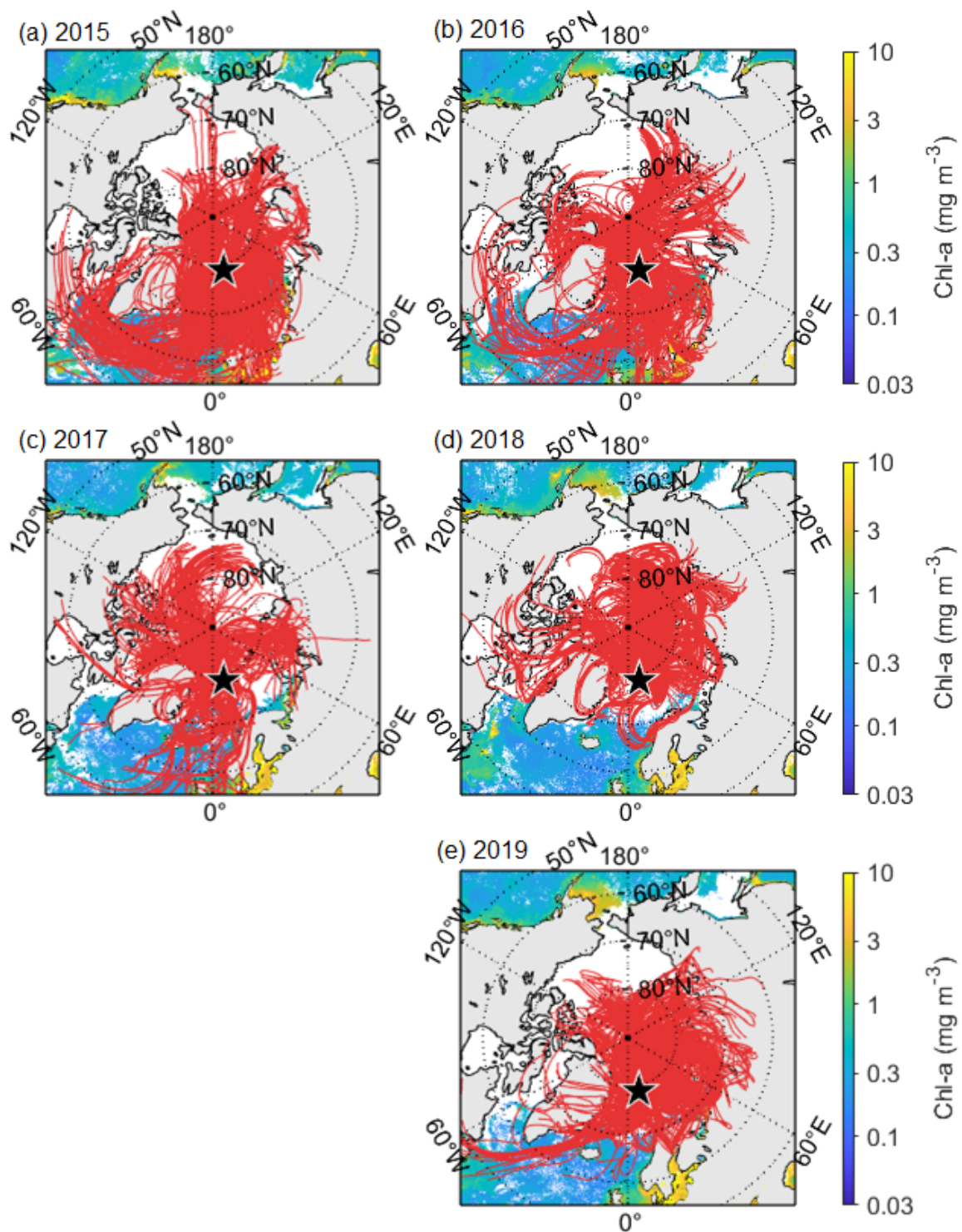


Figure S7: Monthly mean Chl-*a* concentration in each year layered with 5-day air mass back trajectories during March. Black pentagram indicates the location of the sampling site.

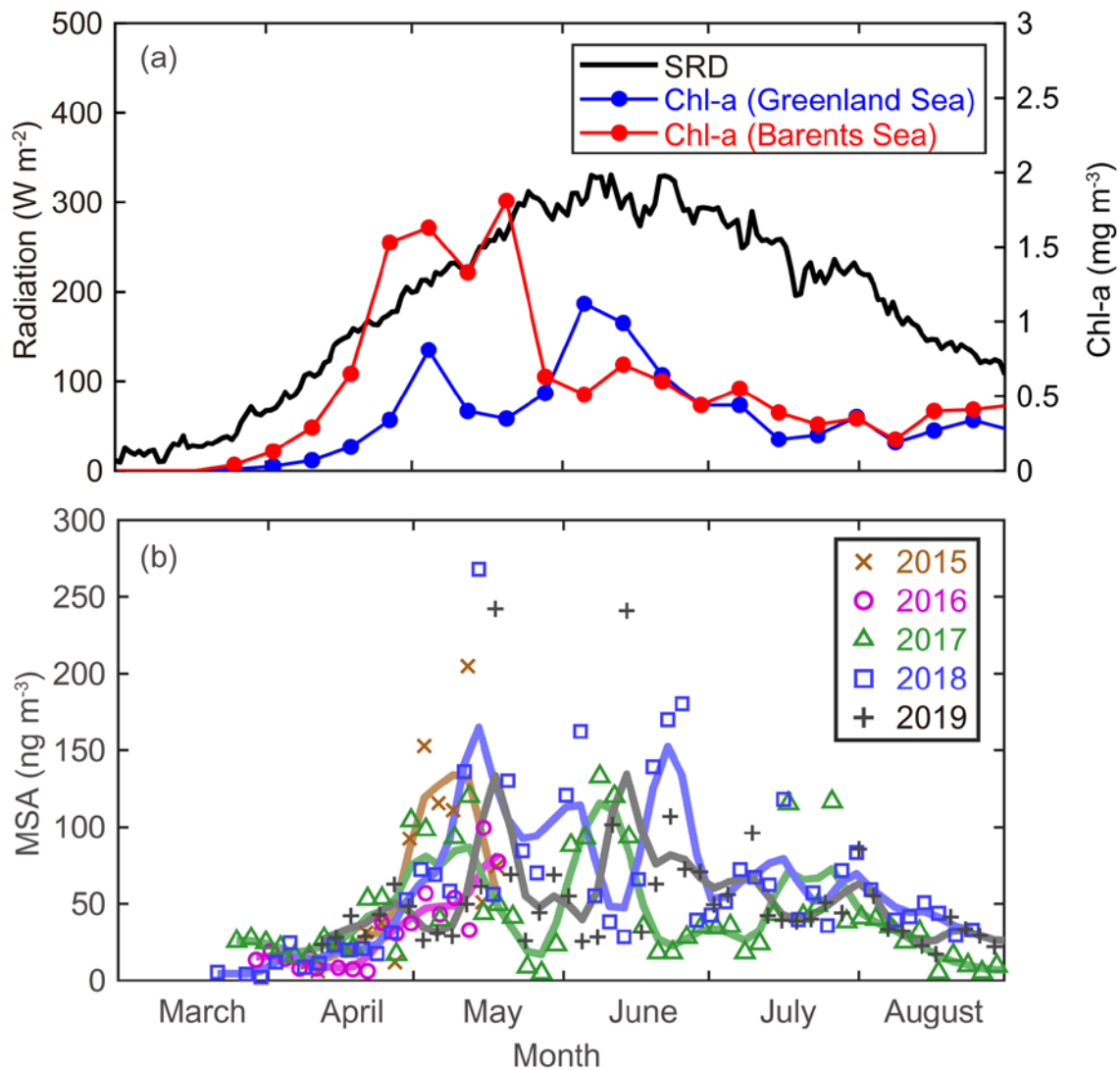


Figure S8: (a) Mean radiation and mean Chl-a concentration in Greenland and Barents Seas, (b) MSA concentration for 2015, 2016, 2017, 2018 and 2019.

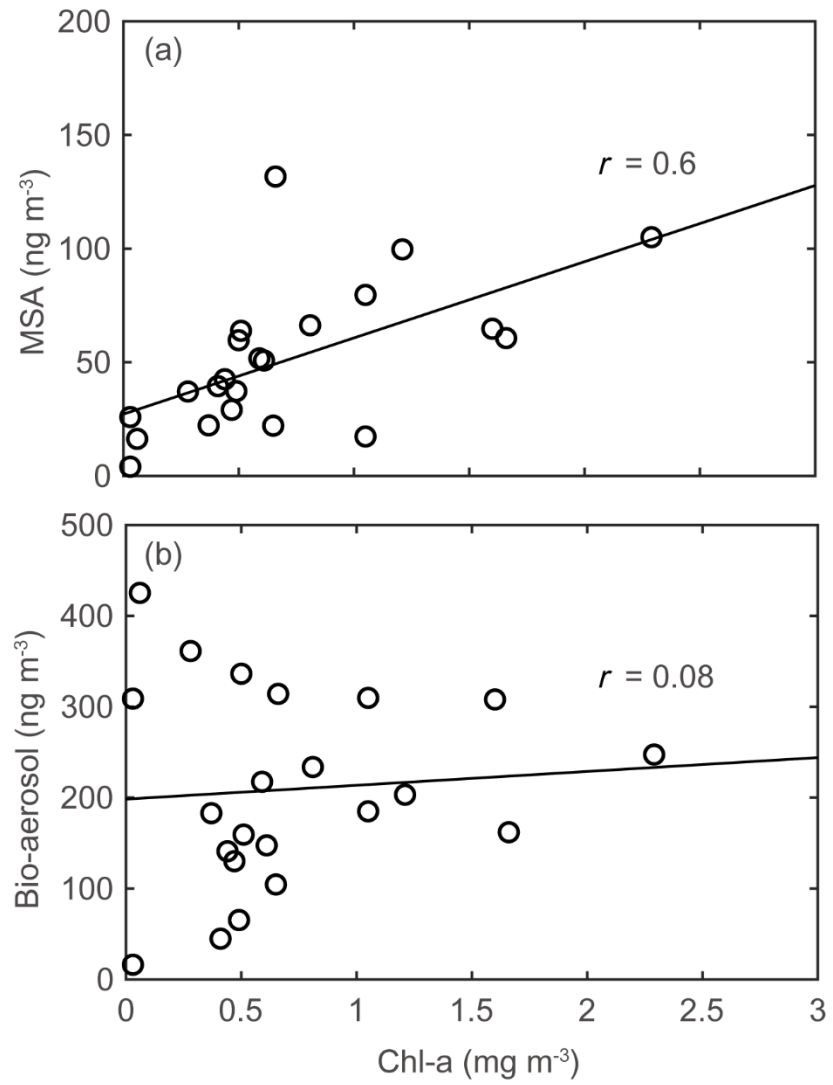


Figure S9: Scatter plot of monthly mean Chl-*a* versus (a) monthly mean MSA and (b) monthly mean Bio-aerosol for 2015, 2016, 2017, 2018 and 2019.

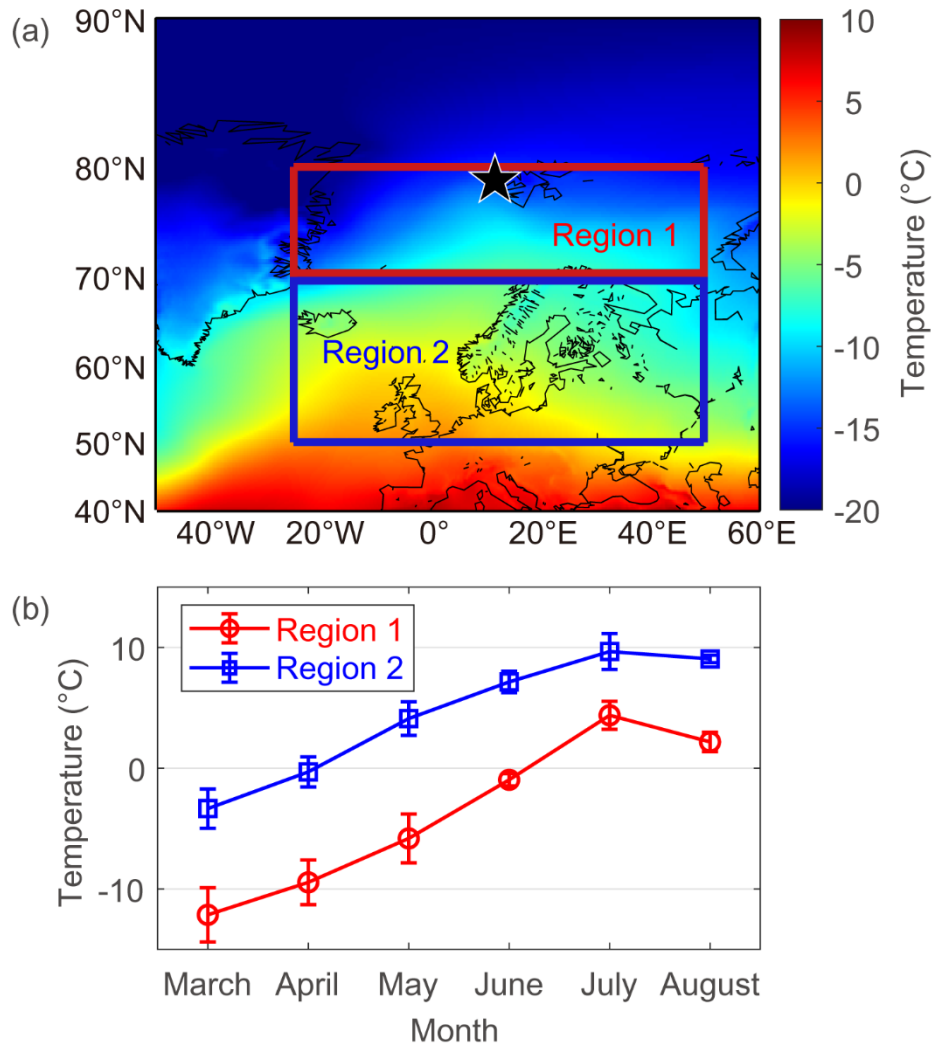


Figure S10: (a) Mean temperature map in March with ocean domains of Greenland & Barents Sea (Region 1; 70° N–80° N, 25° W–50° E), and North Atlantic & Norwegian Seas (Region 2; 50° N–70° N, 25° W–50° E), and (b) mean temperature at 900 hPa from European Centre for Medium-Range Weather Forecasts Reanalysis 5 in different ocean domains during 2015–2019, error bars represent 1σ for 2015, 2016, 2017, 2018 and 2019, respectively.

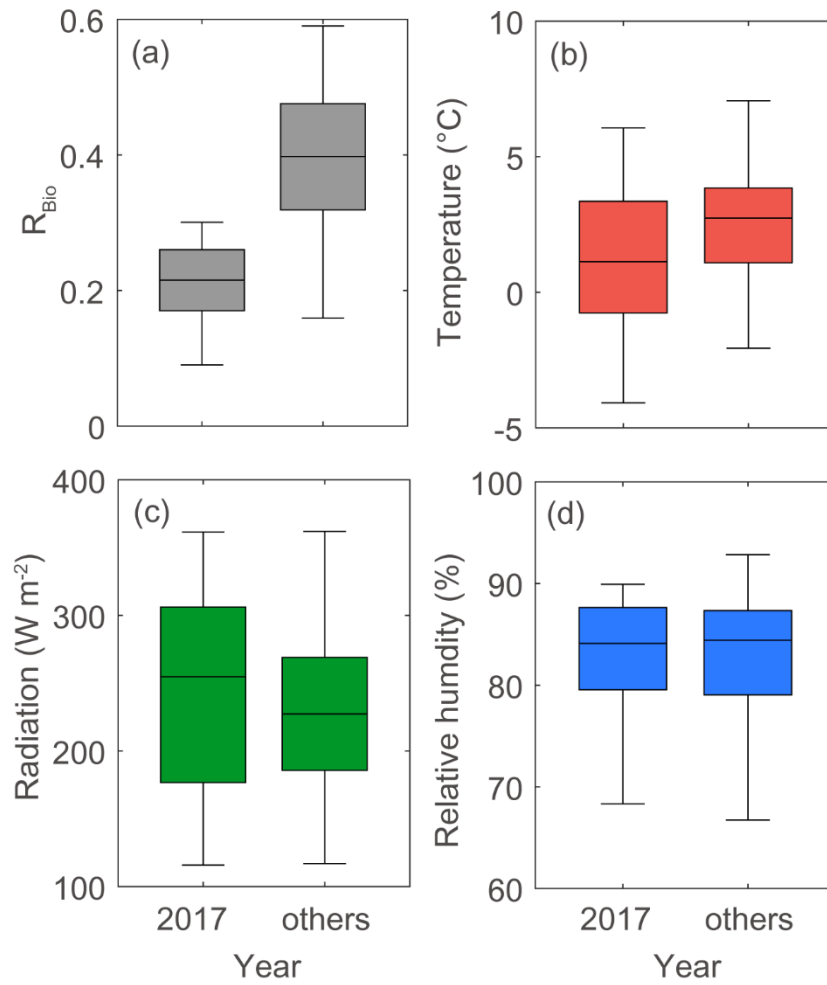


Figure S11: Box plot of (a) R_{Bio} , (b) air mass temperature, (c) radiation, (d) relative humidity during post-bloom period. Meteorological factors were calculated for air masses has been subject to in the 5 days prior to reaching the measurement site at Svalbard. Solid line represents median of each data in box plot.